DOI: 10.1089/ten.tea.2018.0197

SWINE MENISCUS: ARE FEMORAL-TIBIAL SURFACES PROPERLY TUNED TO BEAR THE FORCES EXERTED ON THE TISSUE?

Peretti, GM[1,2], **Polito, U[3]**, Di Giancamillo, M[4], Andreis, ME[3], Boschetti, F[2,5], and Di Giancamillo, A[3]

[1]*Department of Biomedical Sciences for Health, Università degli Studi di Milano, Italy*

[2]*IRCCS, Istituto Ortopedico Galeazzi, Milan, Italy*

[3]*Department of Health, Animal Science and Food Safety, Università degli Studi di Milano, Italy*

[4]*Department of Veterinary Medicine, University of Milan, Italy*

[5]*Department of Chemistry, Material and Chemical Engineering Department "Giulio Natta", Politecnico di Milano*

Abstract

Menisci are subjected to different pathologies that affected the knee proper functions and biology. Over the years, different techniques were tried to repair meniscus injury, and, when the reparation was not possible, to replace or regenerate it.

These techniques still present a lack of controlled and independent clinical studies that not allow identifying their effective failure rate.

This rate could be due to a still incomplete knowledge about meniscal biology, its composition and biomechanical properties.

The purpose of this study was to analyse the relationship between the contact forces and the meniscal structures at the level of the femoral and tibial surfaces of the meniscus to improve the knowledge about this tissue, in view of the possible application in tissue engineering, for the production of meniscal scaffolds. Swine meniscal samples were studied for morphological (Safranin-O, Sirius Red and collagen type I and II), biochemical (DNA, GAGs and GAGs/DNA ratio), CT scanning and biomechanical analyses (compression and traction tests) of femoral and tibial meniscal surfaces. Results revealed a biomechanical-dependent characterization of the meniscus.

The femoral surface is characterized by a higher quantity of GAGs and a greater amount of cells ($p<0.01$ for each analysis), with the interposition of radial and oblique fibres. These features are responsible of a higher resistance ($p<0.05$) to compressive forces like that acted on by the femoral condyles.
Oppositely, the tibial surface shows a circumferential arrangement of the fibres and a poorer GAGs presence and cellular spread ($p<0.01$); these characteristics seem to allow a higher resistance ($p<0.05$) of the tibial surface to traction forces.
Results from this work provide useful information for the design and creation of meniscal substitute and suggest that the features of the meniscus are biomechanical-dependent and that its composition and structure are dependent to the different forces that femur and tibia generate upon its surfaces.
The importance of the present study is linked to how the contact forces act on the knee meniscus in particular considering the femoral condyles and tibial plateau: these results can be useful for the tissue-engineering of meniscus, providing information about meniscal biology, its composition and biomechanical properties.

Keywords: meniscus, swine, anatomy, biomechanics

1. Introduction

The knee joint comprises the meniscus, which is a structure composed of a medial and a lateral component and both located between the corresponding femoral condyle and the tibial plateau [Kohn and Moreno, 1995]. It is a white and glossy complex tissue composed of cells specialized to produce extracellular matrix (ECM). Menisci are characterized by specific regional innervation and vascularization [Di Giancamillo et al., 2014]. Both are critical components of a healthy knee joint [Greis et al., 2002]. Moreover, meniscal tissue comprises a large network of collagen fibrils, which embed the ECM, as well as water. Collagen fibrils networks are indirectly involved in the joint biomechanics by strengthening the tissue fluid pressure under load, and directly by resisting tensile forces [Shirazi et al., 2008]. The collagen fibrils network (considering composition, structure and arrangement) spatially vary within the meniscus along the depth, because collagen is the meniscal element which can contribute to the main function of this tissue itself, i.e. loading transmission [Kaab et al., 1998].
The meniscus bears many different forces such as traction and compression. It also plays a crucial role in the transmission of load, shock absorption, lubrication and nutrition of articular cartilage [Proctor et al., 1989]. All these functions are very complex and require a specialization of the meniscus itself. Since the meniscus structure is wedge-shaped, it is very efficient in stabilizing the round-shaped femoral condyle as well as the flat tibial plate [Sweigart and Athanasiou, 2001].
The contact forces acting on the meniscus inside the knee joint have been extensively studied. It was

between the articular cartilage of the femoral condyles and the tibial plate, while it transmits more than 50% of the total axial load applied to the joint [Noyes and Barber-Westin, 2010].

Menisci are subjected to different pathologies (principally tears and degeneration) that can affect their fundamental functions for the knee joints. It is demonstrated that pathologies of meniscus lead to gonarthrosis, with higher impact on human welfare [Dangelmajer et al., 2017; Guo et al., 2015; Sun et al., 2015]. For these reasons, different techniques were developed during time to try to treat meniscal injuries. The first technique adopted was the meniscectomy [Guo et al., 2015], this technique contemplated the removal, initially, of the whole meniscus, was than partially renovated, trying to diminish, only to whom damaged, the entity of meniscal tissue removed. However, a lack of meniscal tissue was associated to the development of arthrosis and even a partial meniscectomy (that is currently the principal method to treat this pathologies) lead, with different grades, to the same result [Guo et al., 2015]. Then, removal was abandoned, when not necessary, in favour of reparation: different techniques of reparation were developed to treat meniscal injuries [Vaquero and Forriol, 2016], but these kinds of techniques were seen to be functional only in the cases when the lesions affected the peripheral region of meniscus (i.e. the most vascularized [Di Giancamillo et al., 2017] and inclined to regeneration [Vaquero and Forriol, 2016]).

For these reasons, in the past years, the request of new techniques, which lead to the ultimate replacement or regeneration of the meniscus, increased. The focus of these techniques is to restore the knee biomechanics, distribute the load across a larger contact area (compared to meniscectomy) and potentially delayed the onset of osteoarthritis [Dangelmajer et al., 2017].

In the last years, different techniques were developed in this direction, with scaffolds replacements and allograft transplantations [Dangelmajer et al., 2017; Guo et al., 2015; Sun et al., 2015; Vaquero and Forriol, 2016], but due to their relatively new creations, these techniques still present a lack of controlled and independent long-term clinical studies that not allow identifying their effective outcomes [Dangelmajer et al., 2017].

Nevertheless, a certain failure rate is in any case present [Dangelmajer et al., 2017]. Probably, this can be ascribed to a still incomplete knowledge about meniscal biology, its composition and biomechanical properties.

The aim of the present study was to deepen the relationship between the contact forces and the knee structures, in particular to search for the differences between the femoral condyles and tibial plateau surfaces of menisci, as a base for the ultimate creation of tissue-engineered biphasic scaffolds, which can mimic the native tissue complex, for meniscal repair or regeneration.

2. Materials and methods

2.1. Study design

Seen the similarity with human meniscus [Proffen et al., 2012; Deponti et al., 2015] and the huge utilization as model for meniscal tissue engineering [Deponti et al., 2015] and repair [Zhang et al., 2014; Deponti et al., 2015], pig's menisci were chosen as samples for this study. The knee joints of 26 adult (~9 months old) female pigs (Landrace x Large white, average weight 75–90 kg; n=104 meniscal samples) were obtained from a local slaughterhouse and dissected to isolate the tibia and remove the menisci. Capsular tissue and ligaments were removed, and the menisci were sectioned according to the purpose of the study as described below (Fig1). Only joints presenting as healthy at dissection were included in the study. Furthermore, giving the similarities between medial and lateral menisci observed by previous micro-anatomical analysis [Di Giancamillo et al., 2014; Zhang et al., 2014], medial and lateral meniscal samples were pooled for the biochemical and biomechanical analyses. Moreover, limbs from 6 pigs were used for CT scanning as described below. The Ethic Committee of the University of Milan (OPBA, 58/2016) approved the use of cadavers for research purpose; furthermore, all the animals are dead for causes not related with the present study.

2.2 Morphological analyses: histology and immunohistochemistry

Both the medial and lateral menisci (n=28) were transversally sectioned into the three parts, corresponding to the anterior horn, central body and posterior horn (Fig. 1). Menisci were sampled and fixed in buffered 10% formalin (Bio-Optica, Milan, Italy) for 24 h, dehydrated and embedded in paraffin (total number of specimens = 84). Microtome sections (4-µm thickness) were analysed by with Safranin-O staining (SO) for describing both the menisci structure and the GAGs in the matrix as follows [Schmitz et al., 2010]. Other sections were used for Sirius Red staining [Schmitz et al., 2010] and upon the stained samples; the polarized light microscopy was performed to highlight the birefringence of the collagen fibres in order to assess the spatial orientation of the fibres networks.

Finally, sections (Fig1) were used to detect Collagen type I and II as described elsewhere [Di Giancamillo et al., 2014; Di Giancamillo et al., 2017]. Briefly, dewaxed and re-hydrated sections were treated with 5% H2O2 in Phosphate Buffered Saline (PBS, pH 7.4) for 10 minutes, to inhibit non-specific reactivity. Subsequently, sections were incubated with 1:50 rabbit polyclonal anti-Collagen type I (cod. NB600-408; Novus Biologicals, Littleton, CO, USA) or 1:100 mouse monoclonal anti-Collagen type II (cod. 7005; Chondrex, Redmond, WA, USA country) for 24 h at 18–20°C in humid chamber, then washed in PBS, and subsequently treated with the rabbit or mouse EnVision system, respectively, for 120 minutes at room temperature (Dakocytomation, Milan, Italy). Peroxidase activity was detected with diaminobenzidine

(DAB, DakoCytomation) as the substrate. Appropriate washing with PBS was performed between each step, and all incubations were carried out in a moist chamber. All sections were finally weakly counterstained with Mayer's haematoxylin, dehydrated, and permanently mounted and observed with a microscope (Olympus, Opera Zerbo, Milan Italy) equipped with a digital camera, and final magnifications were calculated.

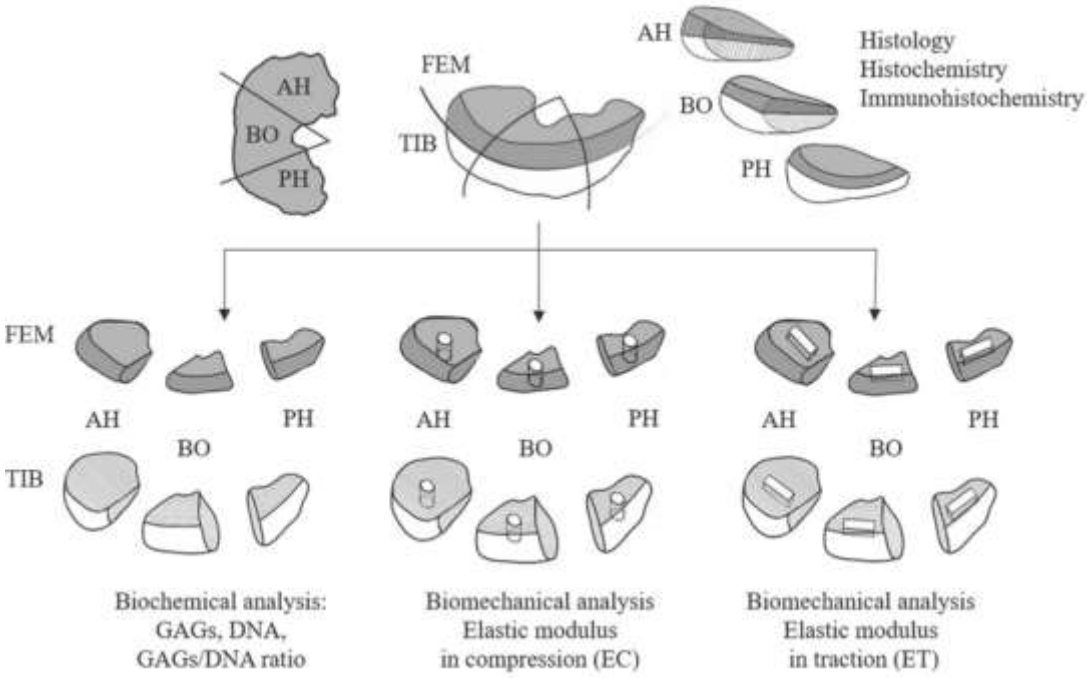

			Portions			
Analysis performed	Menisci (tot: 104)	Sectioning	Anterior Horn (AH)	Body (BO)	Posterior Horn (PH)	Side
Histochemistry and Immunohisto-chemistry	28	Transverse sections	28	28	28	Femoral
			28	28	28	Tibial
Biochemical	20	Transverse & longitudinal sections	20	20	20	Femoral
			20	20	20	Tibial
Biomechanical (EC/ET)	50	Transverse & longitudinal sections	50	50	50	Femoral
			50	50	50	Tibial
Artro-CT	6*	Transverse & longitudinal sections	6*	6*	6*	Femoral
			6*	6*	6*	Tibial
Total	104	*not subdivided				

Fig. 1 Study design. The preparation of the meniscal samples in base of the type of technique performed is shown on the top. The table, on the bottom, resumes the number of each sample utilized for each technique and the type of cuts performed. AH: anterior horn; BO: body; PH; posterior horn. Original picture by U.P.

Biochemical analyses

Sectioned menisci (Fig1, left) of all animals (n=20) were treated as described elsewhere [Di Giancamillo et al., 2017, Sosio et al., 2014; Deponti et al., 2012; Vandeweerd etal., 2011]. Briefly, the samples were digested in papain (Sigma-Aldrich, Milan, Italy) for 16–24 h at 60°C: 125 mg/mL of papain in 100mM sodium phosphate, 10mM sodium EDTA (Sigma-Aldrich), 10mM cysteine hydrochloride (Sigma-Aldrich), 5mM EDTA adjusted to pH 6.5 and brought to 100mL of solution with distilled water. Later, the digested samples were assayed separately for proteoglycan and DNA contents. Proteoglycan content was estimated by quantifying the amount of sulphated glycosaminoglycans using the 1,9-dimethylmethylene blue dye binding assay (Polysciences, Inc., Warrington, PA) and a microplate reader (wavelength: 540 nm). The standard curve for the analysis was generated by using bovine trachea chondroitin sulphate A (Sigma). DNA content was evaluated with the Quant-iT Picogreen dsDNA Assay Kit (Molecular Probes, Invitrogen Carlsbad, CA) and a fluorescence microplate reader and standard fluorescein wavelengths (excitation 485 nm, emission 538 nm, cut-off 530 nm). The standard curve for the analysis was generated using the bacteriophage lambda DNA supplied with the kit.

CT examination

Six hind limbs harvested from pig cadaver were evaluated. Medio-lateral and caudo-cranial radiographs of each stifle were performed to exclude abnormal findings. Each limb was positioned foot-first towards the gantry mimicking dorsal recumbence, with the caudal surface of the limb apposed to the CT couch. Images were acquired with a 16-slices CT scanner (Ge Brightspeed, GE Healthcare – Italy), using a bone algorithm. Scanning parameters were set as follows: kV=120, mA=230, slice thickness=0.625 mm, pitch=0.5625. Each limb was initially positioned in a neutral position. Transverse pre-arthrography CT images were acquired from 2 cm proximal to the patella to 2 cm distal to the tibial tuberosity. Twenty-five ml of iomeprol 150 mg/ml (Iomeron 150, Bracco – Italy) were injected through a 20-gauge hypodermic needle inserted into the stifle joint medial to the mid-point of the patellar tendon [adaptation of the paraligamentous technique described in the ovine stifles, Vandeweerd et al., 2012]. The joint was repeatedly flexed and extended to ensure adequate distribution of contrast medium. The limb was then repositioned on the CT couch and the CT acquisition protocol was repeated. After the acquisition in neutral position, further arthrographic images were acquired with the limb in flexion and in extension. Each limb was flexed and extended as much as manually achievable and secured to the CT couch with large velcro bands (extended: 140±2°; neutral: 116±2°; flexed: 54±4°). The same imaging protocol was then repeated. Images were reviewed by a single radiologist in order to verify meniscal movements, the

contact between femoral/tibial condyles and meniscal surfaces and meniscal compression with different positioning, focusing on the lateral meniscus. Meniscal thickness was measured at the level of the anterior and posterior horn on a MPR (multiplanar reformation) sagittal image passing through the midpoint of the femoral condyle, at a distance of 1 mm from its cranial and caudal surface respectively (Supplementary file1A: red and pink lines). Body portion thickness was evaluated in the same point, as the measure of the midpoint of the meniscus (Supplementary file1A: yellow lines). On the same image, the lengths of the contact surface between the femoral surface of the meniscus and the femoral condyle and between the tibial surface of the meniscus and the tibial condyle were also measured (Supplementary file1B: dark and light blue lines). Finally, the total length of the meniscus was evaluated (Supplementary file1C: green line). All measures were repeated three times for each positioning (extension, neutral, flexion).

Biomechanical testing

Menisci from adult swine (n=50) were stored in saline solution NaCl 0.9% and frozen at -80°C until the time of testing. At least 24 hours before test execution, samples were taken to a temperature of -24°C and then completely thawed at room temperature (23°C). Each meniscus was prepared and cut along the longitudinal axis, in its half height, in order to obtain a meniscal femoral surface and a meniscal tibial surface, too (Fig1). Compression and circumferential traction tests were performed using EnduraTEC ELF® 3200 machine, equipped with a 220 or 22N load cell depending on the test and sample.

For compression tests, 25 menisci were used. Specimens were obtained dividing each meniscal surface in the three portions after the longitudinal cut (Fig1): anterior horn, body and posterior horn (n=75). Subsequently, for each zone, a cylindrical sample perpendicular to the femoral and tibial surfaces was cut using a die cutter (Fig1, in the middle). Before testing, dimensional measurements on the specimens were made with a digital calliper (Mitutoyo Corp, Kanogawa, Japan, number of series 06,081,911, accuracy class 1). The samples were inserted into a Plexiglas cell and PBS solution was added into the cell to avoid dehydration of the specimen during the test. The samples thickness was measured from the position of the testing machine actuator, after imposing a preload of 0.1N. The sample was then subjected to a multi-ramp stress relaxation test, made of five increasing 4% strains at a velocity of 0.1%/s, followed by stress relaxation to equilibrium for 600s. The compressive modulus, Ec, was obtained for each ramp from the equilibrium data as the ratio between values of relaxation stress and the corresponding values of strain.

For circumferential tension test (n=25 menisci), we obtained representative fragments of the meniscus anterior horn, body and posterior horn on both femoral and tibial surfaces (n=75). These fragments were cut out using a scalpel, trying to obtain samples with a shape as similar as possible to a parallelepiped (Fig1, on the right) and following the circumferential tensile force direction. Before testing, dimensional

measurements on the specimens were made with the same digital callipers previously indicated. Width and thickness of each sample were obtained using the callipers, length instead was measured on the mounted specimen, considering as length the distance between the two grips after a preload of 0.1N application. The specimens were subjected to a multi-ramp stress-relaxation test, made of four increasing 4% strains at a velocity of 0.1%/s, followed by stress relaxation to equilibrium for 1200 s. A custom made

Statistical Analysis

Statistical analyses of the biochemical (GAGs, DNA and GAGs/DNA ratio), biomechanical results (compression and traction tests) and CT measures (horns' thickness, body thickness, meniscal length, and femoral and tibial contact surfaces) were analysed with 2-ways ANOVA with surfaces (femoral and tibial surfaces) and meniscal portions (anterior horn, body, posterior horn) as main factors. The statistical analysis was performed using the general linear model of the SAS (version 8.1, Cary Inc., NC). The individual meniscal samples were considered to be the experimental unit of all response variables. The data were presented as least squared means ± SEM. Differences between means were considered significant at $p<0.05$.

Results & Discussion

Morphological analyses: histochemistry and immunohistochemistry

Considering the similarities of the medial and lateral meniscus already described in a previous study of our research group [Di Giancamillo et al., 2014] only data regarding morphology of the lateral meniscus are presented. Safranin-O histochemistry assessed that the amount of matrix (proteoglycans) was more evident in the inner part both in anterior and posterior horns (Fig. 2A, 2B respectively; asterisks), similarly to the results of previous works, that showed the same aspect in the inner part of ovine meniscus [Melrose et al., 2005].

Proteoglycans were also predominant within the anterior horn (Fig. 2A1, 2A3; asterisks) when compared with the posterior one (Fig2: B1, B3; asterisks), and in the femoral meniscal surfaces (Fig. 2A1, 2B1; asterisks) when compared with the corresponding tibial surfaces (Fig 2A3, 2B3; asterisks). Body portion seem to have poorer in GAGs quantity, with a very pale staining in the middle of the tissue (Fig. 2C; asterisk).

These results may suggest a role in the development of the ECM of dynamic compression forces, typically acting on the femoral surface of the meniscus. Moreover, these results suggest, accordingly with a previous work [Di Giancamillo et al., 2014], an earlier development of the meniscal anterior horn with respect to the posterior one. Sirius red stained samples were evaluated to enhance the arrangement of

collagen fibres in the central point of the meniscus.

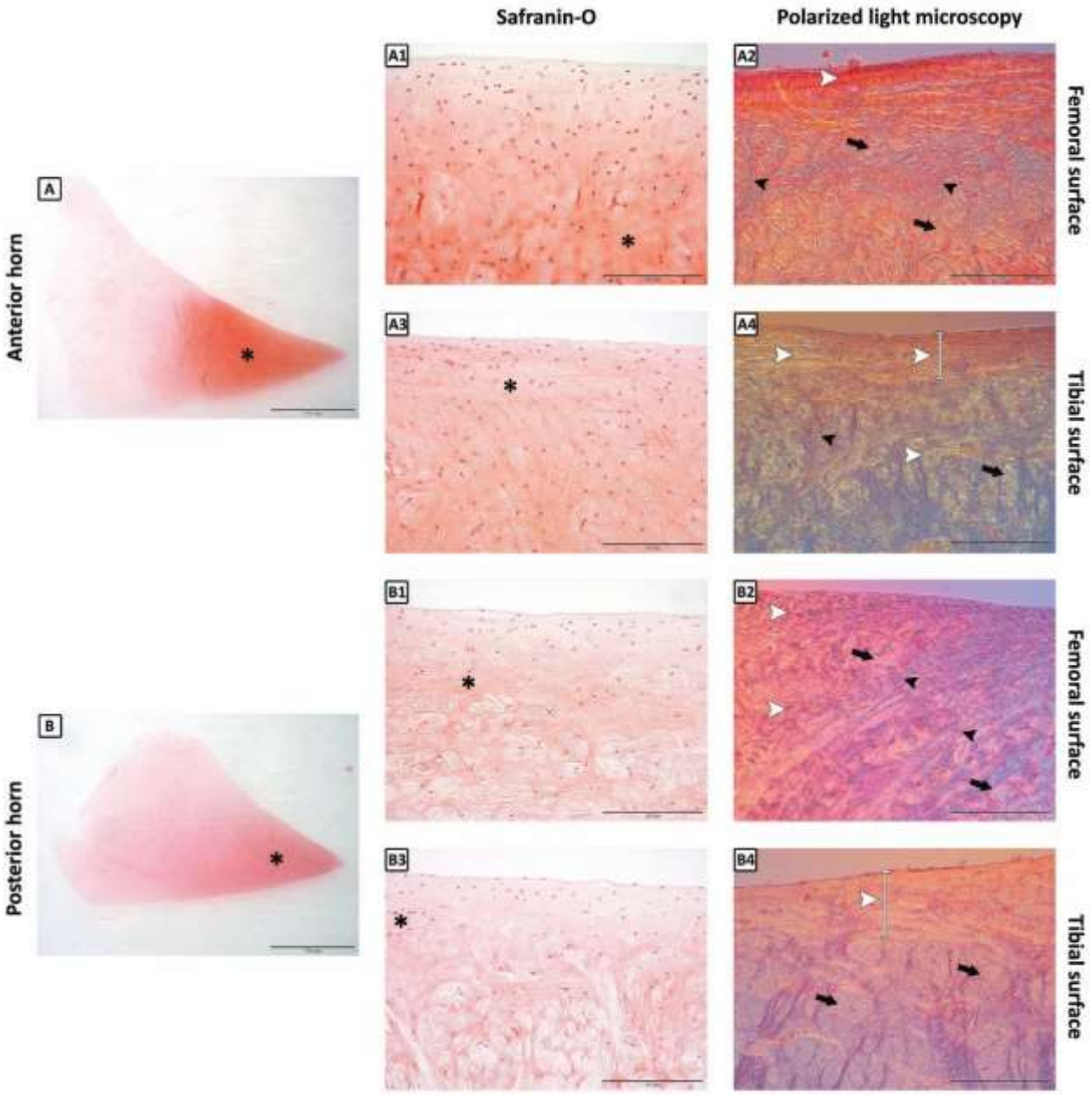

Fig 2. Histochemical findings of the lateral meniscus (Safranin O staining). (A) Anterior horn; (A1) femoral surface; (A3) tibial surface. Body (B): (B1) femoral surface, (B3) tibial surface. Posterior horn (C): (C1) femoral surface; (C3) tibial surface. Histochemical findings of the meniscus (Sirius red staining – polarized light microscopy). Anterior horn: (A2) femoral surface; (A4) tibial surface. Body: (B2) femoral surface, (B4) tibial surface. Posterior horn: (C2) femoral surface; (C4) tibial surface. A, B, Scale bar 5000 µm; A1- A4; B1-B4, Scale bar 200 µm. Black arrows: circumferential fibres; white arrowheads: radial fibres; black arrowheads: oblique fibres; asterisk: matrix deposition.

The spatial disposition of the fibres varied considering the different meniscal portions and regions. The femoral and tibial surfaces of anterior horn presented principally a radial pattern of the fibres in the superficial region, the one closer to the femoral condyle or to the tibial plateau (Fig. 2A2, 2A4; white arrowhead), as seen by other Authors in ovine, human and bovine respectively [AufderHeide and Athanasiou, 2004; Deponti et al., 2012; Vandeweerd et al., 2012; Sosio et al., 2015].

The main differences observed in this study, between femoral and tibial surfaces of the anterior horn were related to a higher incidence of oblique (Fig. 2A2; black arrowheads) and circumferential (Fig. 2A2; black arrows) fibres in the femoral surfaces respect to the tibial ones, while the opposite trend was observed for the radial fibres (Fig. 2A4; white arrowheads). These kinds of fibres recall those observed in the study of Andrews [Andrews et al., 2013] and denominated braided organized type, present in the superficial layer and the woven organized type, present in the deeper layer.

In contrast, the same study (performed upon the anterior horn of bovine medial meniscus) showed no differences between 3D fibres arrangement in the femoral and the tibial surfaces [Andrews et al., 2013].

The posterior horn showed much different patterns between the femoral and tibial surfaces and between the deep and superficial regions of both surfaces. In the superficial femoral surface (the one closer to the femoral condyle), it was possible to recognized two layers of fibres disposed in a radial arrangement (the most superficial one, Fig. 2B2; white arrowhead) and a circumferential arrangement (deeper with respect to the previous, Fig. 2B2; black arrows), while in the deepest region of the femoral surface, there was a wider occurrence of radial (Fig. 2B2; white arrowhead), oblique (Fig. 2B2; black arrowheads) and circumferential fibres (Fig. 2B2; black arrow).

Moreover, the tibial surface of the posterior horn presented a wider radial disposition of the fibres in the superficial region (the ones closer to the tibial plateau, Fig. 2B4; white arrowhead), while in the deepest region there are fibres mostly arranged in a circumferential pattern (Fig. 2B4; black arrow).

Generally, in the posterior horn, femoral and tibial surfaces showed a conventional fibre arrangement, as already described by other works, the differences seen in this paper between the two surfaces differed from those described by those Authors for ovine and bovine menisci, respectively [Deponti et al., 2012, Vandeweerd et al., 2012] but could be grossly assimilate to those reported by AufderHeide and Athanasiou [AufderHeide and Athanasiou, 2004], and Petersen and Tilmann [Petersen and Tilmann, 1998], in human.

Body portion seem to have an intermediate pattern of fibres, with a higher prevalence of circumferential fibres (Fig. 2B2, black arrows) in the femoral surface and a higher disposition in radial (Fig2B4, white arrowhead) direction in the tibial one.

Immunohistochemistry showed a regional dependent matrix deposition: collagen I was present principally in the posterior horn (Fig. 3E1, 3E2, 3E3), in the femoral (Fig. 3E1) and tibial (Fig. 3E2) surfaces of the meniscus and in the inner region (Fig. 3E3). In the anterior horn collagen I was shown only by a nuclear staining (Fig 3A1, 3A2, 3A3; brown in the pictures). Collagen II was present in the anterior horn (for the inner, femoral and tibial parts, Fig. 3B1, 3B2, 3B3) and in the posterior horn (almost only in the inner part, Fig. 3F3). These results agreed with previous work that showed an age-dependent localization of the collagen disposition in ovine and swine [Deponti et al., 2012 and Di Giancamillo et al., 2014, respectively]. Body shows once again an intermediate pattern, with a poor, almost only nuclear, expression of collagen I (as seen in anterior horn, Fig. 3C1, 3C2, 3C3) and a poor expression of collagen II (as seen in posterior horn 3D1, 3D2, 3D3), but a higher presence of collagen II in the inner part respect to the latter (Fig. 3D3, asterisk).

Collagen I, much more abundant in immature meniscal tissue [Di Giancamillo et al., 2014] and tendons [AufderHeide and Athanasiou, 2004], was mainly expressed by the posterior horn (Fig. 3E1, 3E2, 3E3) that, as seen previously [Di Giancamillo et al., 2014] developed later with respect to the anterior one. On the other hand, collagen II, much more abundant in mature meniscal tissue [Di Giancamillo et al., 2014] and cartilage [AufderHeide and Athanasiou, 2004] was expressed in the anterior horn (Fig. 3B1, 3B2, 3B3) which developed earlier in the meniscal tissue. Note that only the inner, and, much compressed, part of the posterior horn expressed collagen II in its matrix (Fig. 3F3). Once again, these results showed how biomechanical forces are essential for the right development of the meniscal structure.

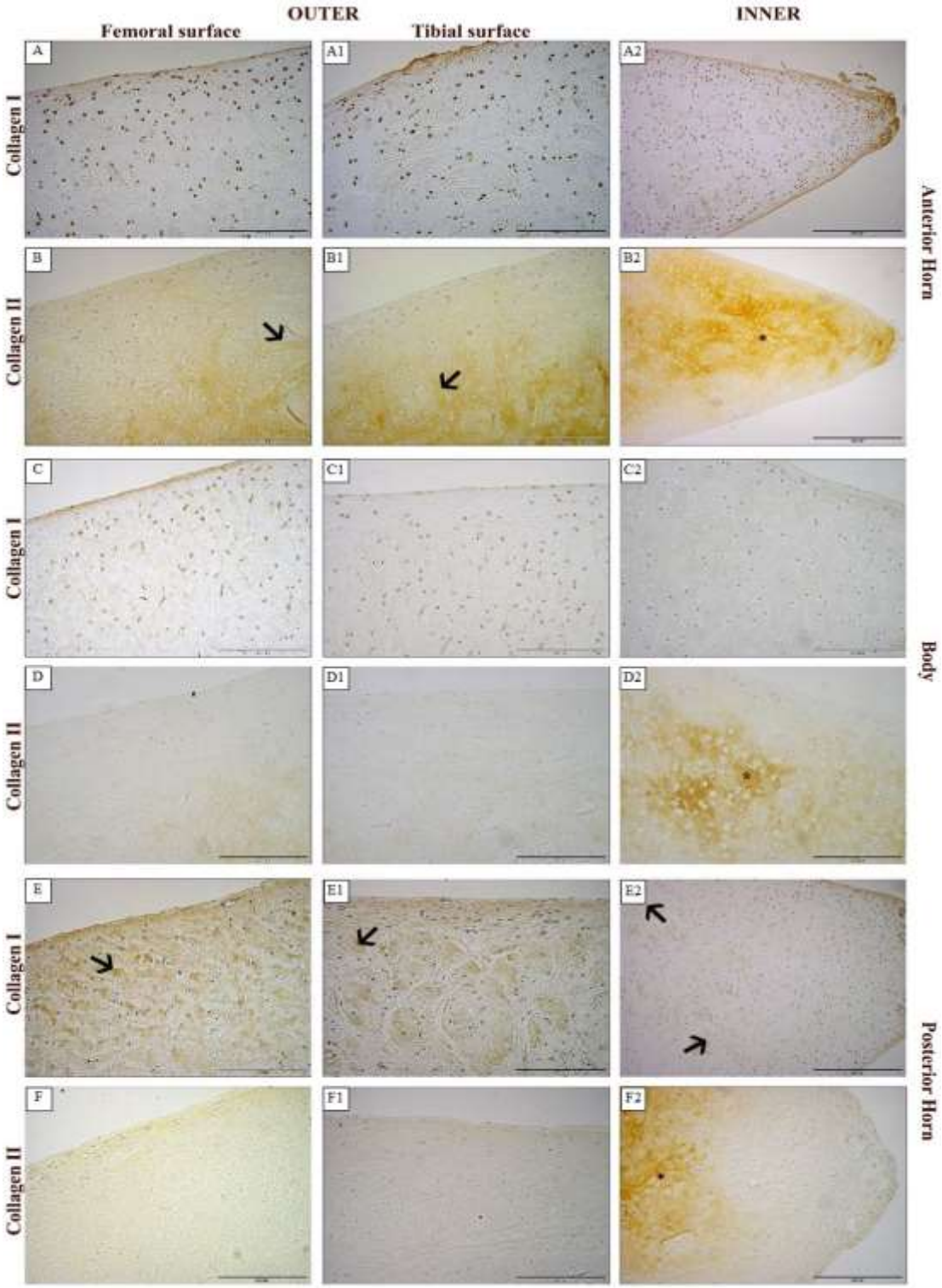

Fig. 3 Immunohistochemistry for collagen type I of the lateral meniscus: Anterior horn: (A1) Femoral surface; (A2) tibial surface; (A3) inner part. Body: (C1) Femoral surface; (C2) tibial surface; (C3) inner part. Posterior horn: (E1) Femoral surface; (E2) tibial surface; (E3) inner part. Immunohistochemistry for collagen type II. Anterior horn: (B1) Femoral surface; (B2) tibial surface; (B3) inner part. Body: (D1) Femoral surface; (D2) tibial surface; (D3) inner part. Posterior horn: (F1) Femoral surface; (F2) tibial surface; (F3) inner part. Arrows: fibers; asterisk: matrix deposition. All the figures have the same scale bar: 100 µm.

3.2. Biochemical analysis

Biochemical analysis quantified the cellular spread and the GAGs amount through the meniscal tissue.

Both DNA and GAGs contents were higher in the femoral surface ($p<0.05$) when compared with the tibial one (Fig. 4A, 4B), while the GAGs/DNA ratio showed no significant differences, but a higher value for the femoral surface (Fig. 4C).

In particular, DNA content was higher in both anterior and posterior horns of the femoral surface when compared with the corresponding tibial surface portions (Fig. 4A; $p<0.01$ and $p<0.05$, respectively). Body portions of both femoral and tibial surfaces presented no statistically significant differences (Fig. 4A).

A similar trend was present in GAGs quantification, that is characterized by a higher value in both anterior and posterior horns of the femoral side when compared with the corresponding tibial portions (Fig 4B; $p<0.01$). GAGs quantification showed also a poorer ($p<0.05$) statistically significant difference between the femoral and tibial body portion, with a higher value present in the femoral surface (Fig 4B).

GAGs were evaluated to analyse matrix content in relation with the response to compressive forces as observed by Bursac et al. (2009) in human and by Abdelgaied et al. (2015) in pigs.

The GAGs/DNA ratio showed no significant differences among all portions (Fig4F). This may be due to the fact that adult meniscus had reached a complete development, and so, cells, matrix and collagen network, achieved an equilibrate connection throughout the entire tissue, differently from what could be seen in growing menisci [Abdelgaied et al., 2015].

Biochemical analysis reiterated, once again, the presence of two well-differentiated portions: a femoral (rich of cells and glycosaminoglycans) and a tibial one (characterized by the greater relative amount of fibres). The obtained data were in agreement with previous description of the meniscus as a tissue having an inner proteoglycan rich matrix [AufderHeide and Athanasiou, 2004, 31] that resembles hyaline cartilage and an external fibrous region, more similar to ligament and tendons [Moon et al., 1984; Cheung, 1987; AufderHeide and Athanasiou, 2004; Son et al., 2012].

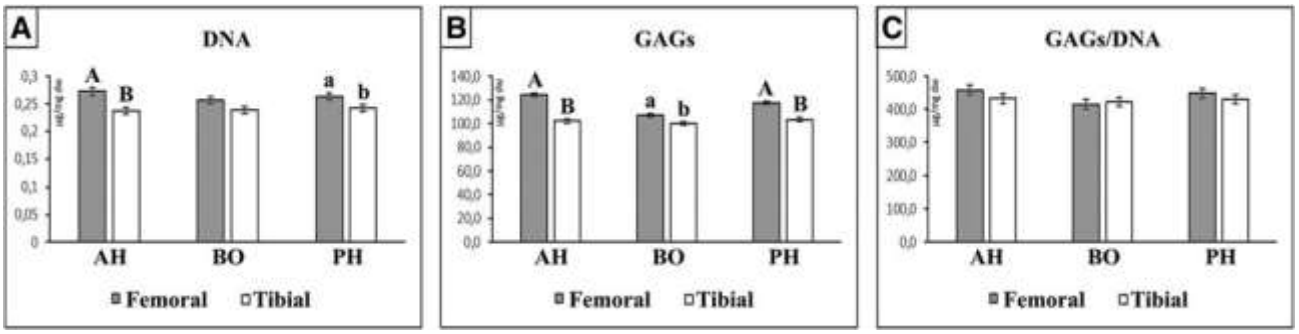

Fig 4 Biochemical analysis results. DNA, GAGs and GAGs/DNA ratio (A, B and C) are shown. DNA values (i.e. cellularity, A) and GAGs quantification (B) are higher among the femoral meniscal contact surface when compared with the tibial one. Values with different subscripts (a, b) for $p< 0.05$ and (A, B) for $p< 0.01$.

3.3. CT scanning

The results of CT analysis (Fig. 5) provided a hint of meniscal behaviour during knee's movement. During standing and movement, neutral positioning corresponded to full loading, while flexion corresponded to general stifle unloading [Fuss, 1991]. The thickness of the meniscus in different positioning seemed to suggest that compressive forces on the anterior horn, body and posterior horns (Fig. 5D) have no effects upon their macroscopic structure. The same happened for the total length of the meniscus (Fig. 5E), as their complex structure allows them to hold their shape under different stimuli. Flexion seemed to induce a noticeable reduction in the length of the contact surface among the meniscus and both the bone surfaces (for both, $p<0,01$; Figs. 5A-C, 5F and 5G). However, the femoral contact surfaces seemed to be less affected by the extension (Fig. 5F; $p<0,05$) and the tibial contact surface seemed to be not affected at all (not statistically significant respect to the neutral position, Fig. 5G). A large amount of contrast medium seemed to fill the space between the anterior horn of the meniscus and the femoral and tibial condyles (femur > tibia), suggesting a fan-like separation between the horn and the bone surfaces during flexion (Fig. 5C; red arrows). Moreover, caudal displacement of the meniscus was visible, which seemed to slip caudally along the tibial condyle (Fig. 5C, yellow arrow) as it was described by other Authors [Fowlie et al., 2011 and Masouros et al., 2010].

The observed differences were related to the decreasing contact between the cranial horn of the meniscus and the two joint heads, while the contact of the caudal horn seemed to be less influenced by the joint movement (Fig. 5A-C).

3.4. Biomechanical tests

Results of biomechanical tests showed a higher compression Elastic modulus (Ec) in the femoral surface with respect to the tibial one (Fig 6A). In particular, anterior and posterior horns presented higher Ec moduli in the femoral surfaces respect to tibial one (Fig 6A; $p<0.05$) while no differences were recorded for the bodies.

The influence of GAGs on tissue compressive force response has been previously demonstrated by other Authors both in human and pigs [respectively Bursac et al., 2009 and Abdelgaied et al., 2015].

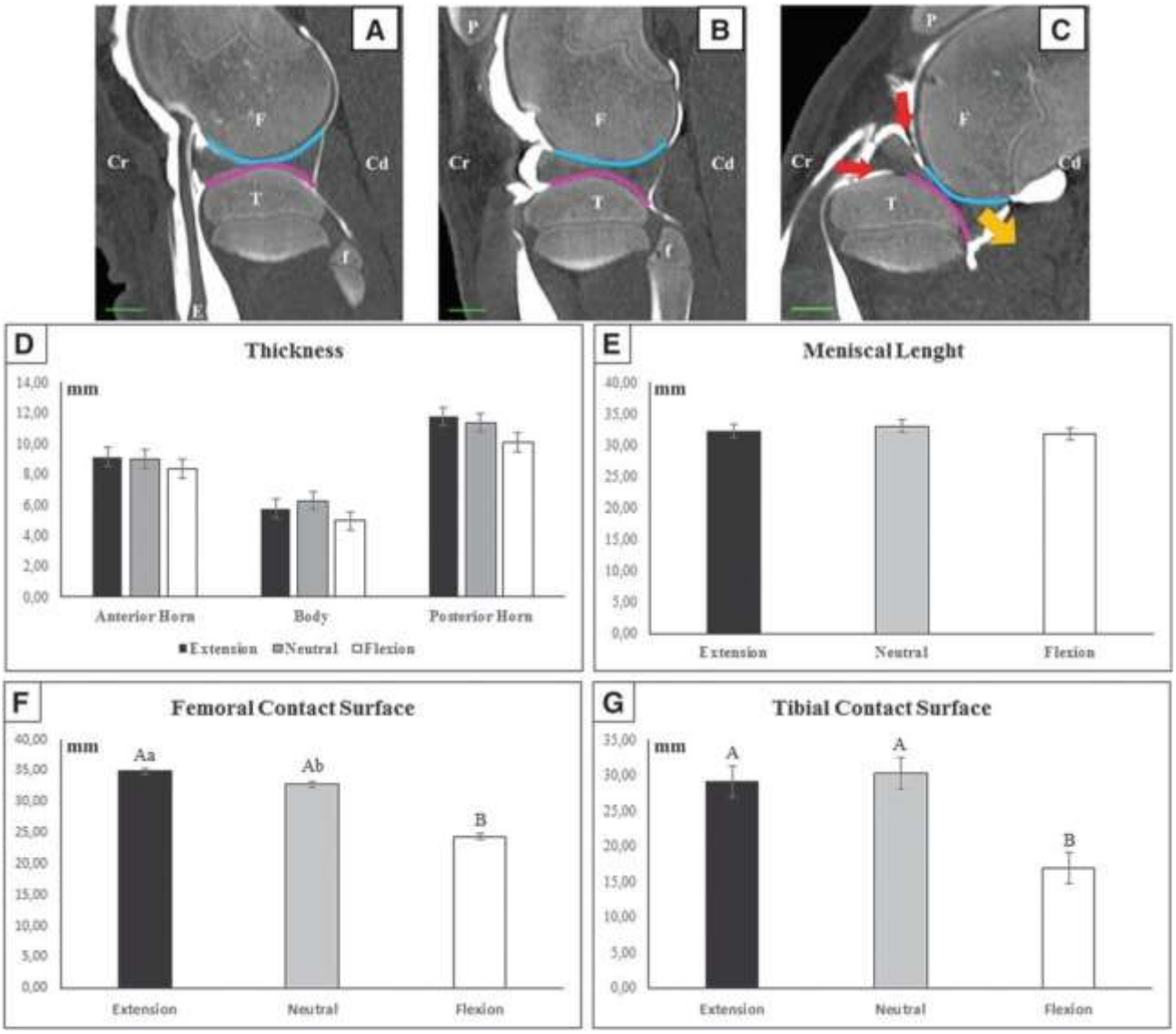

Fig. 5 CT images analysis. Representative images of meniscal changes with different positioning (lateral meniscus): A) in extension,B) neutral, C) in flexion. CT images analysis shows no statistically significant differences both for body and horns' thickness (D) and meniscal length (E) while a reduction in bone/meniscus contact surfaces is evident in flexion (F and G). Contrast mean is noticed between the meniscus and the femoral and tibial surfaces (red arrows), suggesting a fan-like separation of the cranial part of the meniscus from the bones. Caudal displacement of the meniscus along the tibial condyle is also evident (emphasized by the yellow arrow). Values with different subscripts (a, b) for $p<0,05$ and (A, B) for $p<0,01$. Scale bar=1 cm.

In contrast with our results, Proctor et al. (1989), did not find any differences in unconfined elastic modulus in compression, moving from femoral superficial to deeper regions in bovine medial meniscus [Lai and Levenston, 2010]. A higher Ec modulus in the anterior horn (at 12% strain) with respect to the posterior one, was reported by Chia and Hull (2008), in human meniscus. Unfortunately, both these studies did not consider the differences between femoral and tibial surfaces. On the other hand, it was

possible to observe opposite results for what concerned the traction elastic modulus (Et) with a higher value for the tibial surface respect to the femoral one (Fig 6B). It is well known that the Et property is dependent on collagen [Abraham et al., 2011]. In particular, all the three regions (anterior horns, posterior horns and bodies) presented higher values of Et in the tibial surfaces with respect to the femoral ones (Fig 6B; $p<0,05$ for all comparisons). These results showed a different biomechanical behaviour in the different regions and surfaces of the meniscus related to the type of forces the act upon them.

Tensile properties of the meniscus are related with the collagen fibres presence and disposition [Abdelgaied et al., 2015]. A higher tensile modulus value of the anterior horn was also reported by other studies [Kalhon et al., 2015] in porcine meniscus. However, in a study, performed on bovine meniscus, the highest value of tensile modulus was measured in the posterior horn [Proctor et al., 1989; Abraham et al., 2011]. Therefore, these differences may be due simply to interspecific features, but their importance has to be better evaluated in the future.

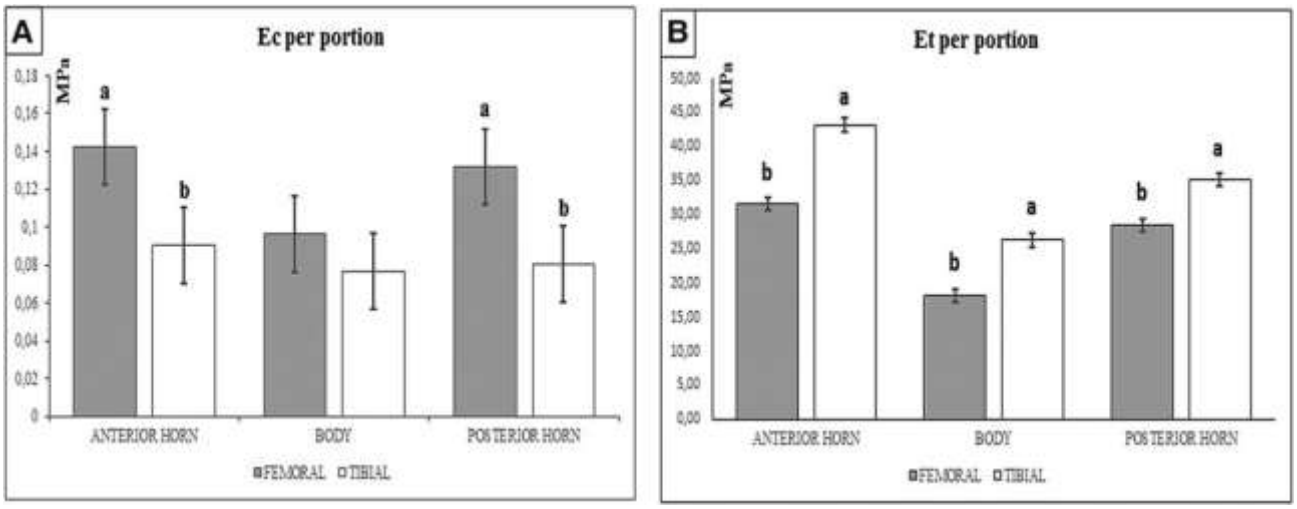

Fig 6 Biomechanical results. Compression test results (A) and Circumferential traction test results (B). Femoral meniscal contact surface shows a higher elastic modulus in compression (Ec; A) while tibial meniscal contact surface shows a higher elastic modulus in traction (Et; B). Values with different superscripts (a, b) for $p < 0.05$.

Biomechanical results draw a picture that characterized the femoral surfaces like more subjected to compressive forces (as previously suspected based on the GAGs presence enhanced by the safranin-O staining and GAGs biochemical quantification), while the tibial surfaces, in particular that of the anterior horn, like more subjected to traction forces. In fact, during physiological loading, tensile, compressive,

and shear forces are generated. Consequently, vertical and horizontal forces result from the femur compressive action on the curved superior surface of the meniscus. From the horizontal force originated a radial reaction force: when the femur compresses the meniscus, it tends to deform radially, but, because of its anchorages to the tibial plateau, it generates a tensile hoop stress resulting from the radial deformation [Athanasiou and Sanchez-Adams, 2009; Muir et al., 2017].

The role of biomechanical forces is essential in the morpho-functional development of the synovial joints components and in particular, for the meniscus, in fact, it was demonstrated that the immobilization of the embryo's hind limb causes the degeneration and the disappearance of this structure [Mikic et al., 2000].

Conclusion

Morphological, biochemical, CT imaging and biomechanical analysis highlight the presence of two well-differentiated meniscal components: a femoral (rich of cells and glycosaminoglycans) and a tibial one (characterized by a greater amount of circumferential fibres). Their different compositions reflect their natural functions: femoral surface act as the springs of a car in response to the transmission of the compressive weight-bearing loads, consequently the tibial surface acts to dissipate the compressive forces, through the collagen fibres network with a hoop-stress mechanism, comparable to car dampers. These functions are biomechanical-dependent and linked to the fibres organization: compressive forces, due to the femoral condyles compression, sliding and rolling, induce a higher deposition of ECM, as well as a circumferential arrangement of the fibres associated with the interposition of some radial and oblique fibres in the corresponding surface of the meniscus. Moreover, traction forces are highly active on the tibial surfaces of the meniscus inducing a circumferential deposition of fibres, which are highly resistant to traction.

Results from this work, even if preliminary, provide useful information for the design and creation of meniscal substitute and suggest that the features of the meniscus are biomechanical-dependent and that its composition and structure are dependent to the different forces that femur and tibia generate upon its surfaces.

Acknowledgments

This paper was supported by the Italian Ministry of Health.

Conflict of interest

Authors declare that they do not have any conflict of interest for the present study.

References:

Abdelgaied, A, Stanley, M, Galfe, M, Berry, H, Ingham, E, and Fisher, J. (2015) *Comparison of the biomechanical tensile and compressive properties of decellularised and natural porcine meniscus*. Journal of Biomechanics 48, 1389–1396. http://dx.doi.org/10.1016/j.jbiomech.2015.02.044

Abraham, AC, Moyer, JT, Villegas, DF, Odegard, GM, and Haut Donahue, TL. (2011) *Hyperelastic properties of human meniscal attachments*. Journal of Biomechanics. 44, 3, 413-8

Andrews, HJ, Ronsky, JL, Rattner, JB, Shrive, NG, and Jamniczky, HA. (2013) *An evaluation of meniscal collagenous structure using optical projection tomography*. BMC Medical Imaging. 13, 21

Athanasiou, KA, and **Sanchez-Adams**, J. (2009) *Engineering the Knee Meniscus: Synthesis Lectures on Tissue Engineering*. San Rafael, Morgan & Claypool Publishers. 1–97.

AufderHeide, AC, and **Athanasiou**, KA. (2004) *Mechanical Stimulation toward tissue engineering of the knee meniscus*. Annals of Biomedical Engineering. 32, 8, 1161-1175.

Bursac, P, Arnoczky, S, and York, A. (2009) *Dynamic compressive behavior of human meniscus correlates with its extra-cellular matrix composition*. Biorheology. 46, 3, 227-237. DOI: 10.3233/BIR-2009-0537

Chen, J, Zhang, L, Sui, X, Xu, W, and Guo, Q. (2015) *Advance and prospects in tissue-engineered meniscal scaffolds for meniscal regeneration*. Stem Cells Int. article ID 517520, hppt://dx.doi.org/10.1155/2015/517520.

Cheung, HS. *Distribution of type I, II, III and V in the pepsin solubilized collagens in bovine menisci*. (1987) Connect Tissue Res. 16, 343–56.

Chevrier, A, Nelea, M, Hurtig, MB, Hoemann, CD, and Buschmann, MD. (2009) *Meniscus structure in human, sheep, and rabbit for animal models of meniscus repair*. J Orthop Res. 27: 1197–203. https://doi.org/10.1002/jor.20869

Chia, HN, and **Hull**, ML. (2008) *Compressive Moduli of human medial meniscus in the axial and radial directions at equilibrium and at a physiological strain rate*. J Orthop. Res. 26, 7, 951- 956. doi: 10.1002/jor.20573

Dangelmajer, S, Familiari, F, Simonetta, R, Kaymakoglu, M, and Huri, G. (2017) Meniscal Transplants and Scaffolds: A Systematic Review of the Literature. Knee Surgery & Related Research. 29, 1, 3-10. doi:10.5792/ksrr.16.059

Deponti, D, Di Giancamillo, A, Mangiavini, L, Pozzi, A, Fraschini, G, Sosio, C, Domeneghini, C, and Peretti, GM. (2012). *Fibrin-based model for cartilage regeneration: tissue maturation from in vitro to in vivo*. Tissue Engineering part A 11(11-12):1109-1122. ISSN: 2152-4955.

Deponti, D, Di Giancamillo, A, Scotti, C, Peretti, GM, and Martin, I. (2015) *Animal models for meniscus repair and regeneration*. J Tissue Eng Regen Med 9: 512–527. DOI: 10.1002/term.1760

Di Giancamillo, A, Deponti, D, Addis, A, Domeneghini, C, and Peretti, GM. (2014) *Meniscus maturation in the swine model: changes occurring along with anterior to posterior and medial to lateral aspect during growth*. Journal of Cellular and Molecular Medicine. 10, 1964-1974.

Di Giancamillo, A, Mangiavini, L, Tessaro, I, Marmotti, A, Scurati, R, and Peretti, GM. (2016) *The meniscus vascularization: the direct correlation with tissue composition for tissue engineering purposes*. J Biol Regul Homeost Agents. Oct-Dec;30 (4 Suppl 1):85-90.

Di Giancamillo, A, Deponti, D, Modina, SC, Tessaro, I, Domeneghini, C, and Peretti, GM. (2017) *Age-related modulation of angiogenesis-regulating factors in the swine meniscus*. Journal of Cellular and Molecular Medicine. 21, 11, 3066–3075.

Fowlie, JG, Arnoczky, SP, Stick, JA, and Pease, AP. (2011) Meniscal translocation and deformation throughout the range of motion of the equine stifle joint: an in vitro cadaveric study. Equine Veterinary Journal. 43, 3, 259-64.

Fuss, FK. (1991) *Anatomy and function of the cruciate ligaments of the domestic pig (Sus scrofa domestica): a comparison with human cruciates*. Journal of Anatomy. 178, 11-20.

Greis, PE, Bardana, DD, Holmstrom, MC, and Burks, RT. (2002) *Meniscal injury: I. Basic science and evaluation*. Journal of American Academy of Orthopaedic Surgery. 10, 3, 168-76.

Guo, W, Shuyun, L, Zhu, Y, Yu, C, Lu, S, Yaun, M, Gao, Y, Huang, J, Yuan, Z, Peng, J, Wang, A, Wang, Y, Sun, J, Vijayavenkataraman, S, and, Liu, H. (2017) *An Overview of scaffold design and fabricatin technology for engineered knee meniscus*. Materials. 10, 29. doi: 10.3390/ma10010029.

Kaab, MJ, Gwynn, IA, and Notzli, HP. (1998) *Collagen fibre arrangement in the tibial plateau articular cartilage of man and other mammalian species*. Journal of Anatomy, 193, 23–34.

Kalhon, A, Hurtig, MB, and Gordon, KD. (2015) *Regional and depth variability of porcine meniscal mechanical properties through biaxial testing*. J Mech Behav Biomed Mater. 41, 108-14. doi: 10.1016/j.jmbbm.2014.10.008.

Kohn, D, and **Moreno**, B. (1995) *Meniscus insertion anatomy as a basis for meniscus replacement: a morphological cadaveric study.* Arthroscopy. 11, 1, 96-103.

Lai, JH, and **Levenston**, ME. (2010) *Meniscus and cartilage exhibit distinct intra-tissue strain distributions under unconfined compression*. Osteoarthritis and Cartilage. 18, 10, 1291-1299. https://doi.org/10.1016/j.joca.2010.05.020

Makris, EA, Hadidi, P, and Athanasiou, KA. (2011) *The knee meniscus: structure-function, pathophysiology, current repair techniques, and prospects for regeneration*. Biomaterial. 32, 30, 7411–7431.

Masouros, SD, Bull, AMJ, and Amis, AA. (2010) *Biomechanics of the knee joint*. Orthopaedic Trauma. 24, 2, 84–91.

Melrose, J, Smith, S, Cake, M, Read, R, and Whitelock, J. (2005) *Comparative spatial and temporal localisation of perlecan, aggrecan and type I, II and IV collagen in the ovine meniscus: an ageing study*. Histochemistry and Cell Biology. 124, 3-4, 225-35.

Mikic, B, Johnson, TL, Chhabra, AB, Schalet, BJ, Wong, M, and Hunziker, EB. (2000) *Differential effects of embryonic immobilization on the development of fibrocartilaginous skeletal elements*. Journal of Rehabilitation Research and Development. 37, 2, 127-133.

Moon, MS, Kim, JM, Ok, IY. (1984) *The normal and regenerated meniscus in rabbits. Morphologic and histologic studies*. Clin Orthop Relat Res.; 182, 264–9.

Muir, P, Pozzi, A, and Cook, JL. (2017) *Meniscal Structure and Function. In Advances in the Canine Cranial Cruciate Ligament*. P. Muir (Ed.). chapter 4, doi:10.1002/9781119261728.ch4

Noyes, FR, and **Barber-Westin**, SD. (2010) *Repair of complex and avascular meniscal tears and meniscal transplantation*. Journal of Bone and Joint Surgery. 92, 4, 1012-29.

Petersen, W, and Tilmann, B (1998). *Collagenous fibrils texture of the human knee joint menisci*. Anat Embryol (Berl) 197, 317-24.

Proctor, CS, Schmidt, MB, Whipple, RR, Kelly, MA, and Mow, VC. (1989) *Material properties of the normal medial bovine meniscus*. Journal of Orthopaedic Research, 7, 6,771-82.

Proffen, BL, McElfresh, M, Fleming, BC, and Murray, MM. (2012) *A comparative anatomical study of the human knee and six animal species*. The Knee. 19, 493–499.

Schmitz, N, Laverty, S, Kraus, VB, and Aigener, T. *Basic Histopathology of joint tissue*. Osteoarthritis and Cartilage. 18, S113-116.

Shirazi, R, Shirazi-Adl, A, and Hurtig, M. (2008) *Role of cartilage collagen fibrils networks in knee joint biomechanics under compression*. Journal of Biomechanics. 5, 41, 16, 3340-8.

Skaggs, DL, Warden, WH, and Mow, VC. (1994) *Radial tie fibers influence the tensile properties of the bovine medial meniscus*. 12, 2, 176-185. https://doi.org/10.1002/jor.1100120205.

Son, M., and **Levenston**, ME. (2012) *Discrimination of meniscal cell phenotypes using gene expression profiles*. Eur Cell Mater. 23, 195–208.

Sosio, C, Di Giancamillo, A, Deponti, D, Gervaso, F, Scalera, F, Melato, M, Campagnol, M, Boschetti, F, NOnis, A, Domeneghini, C, Sannino, A, Peretti, GM. (2015) *Osteochondral Repair by a Novel Interconnecting Collagen-Hydroxyapatite Substitute: A Large-Animal Study*. TISSUE ENGINEERING PART A 21, 3-4, 704-715.

Sweigart, MA, and **Athanasiou**, KA. (2001) *Toward tissue engineering of the knee meniscus*. Tissue Engineering, 7, 2, 111-29.

Vaquero, J, and **Forriol**, F. (2016) *Meniscus tear surgery and meniscus replacement*. Muscles, Ligaments and Tendons Journal. 6 (1):71-89.

Vanderploeg, EJ, Wilson, CG, Imler, SM, Ling, CH-Y, and Levenston, ME. (2012) *Regional variations in the distribution and colocalization of extracellular matrix proteins in the juvenile bovine meniscus*. J. Anat. 221, pp174–186. doi: 10.1111/j.1469-7580.2012.01523.x

Vandeweerd, JM, Kirschvink, N, Muylkens, B, Depiereux, E, Clegg, P, Herteman, N, Lamberts, M, Depiereux, E, Clegg, P, Bonnet, P, Nisolle, J-F. (2012) *A study of the anatomy and injection techniques of the ovine stifle by positive contrast arthrography, computed tomography arthrography and gross anatomical dissection*. The Veterinary Journal. 193. 426–432. doi:10.1016/j.tvjl.2011.12.011

Zhang, X, Aoyama, T, Ito, A, Tajino, J, Nagai, M, Yamaguchi, S, Iijima, H, and Kuroki, H. (2014) *Regional Comparisons of porcine menisci*. J Orthop Res. 32, 1602–1611. doi:10.1002/jor.22687.

Supplementary file 1 CT measures (lateral meniscus). A. Meniscal thickness at the level of the anterior horn (red line), body (yellow line) and posterior horn (pink line). B. Length of the contact area between the femoral surface of the meniscus and the femoral condyle (dark blue line) and between the tibial surface of the meniscus and the tibial condyle (light blue line). C. Total meniscal length (green line). P=patella; F=lateral femoral condyle; T=lateral tibial condyle; f=fibula; Cr=cranial; Cd=caudal.MPR image reconstructed on a sagittal plane passing through the midpoint of the lateral femoral condyle (neutral positioning). Bar=1 cm.